

Green Synthesis of Zinc Sulfide Nanoparticles for the Removal of Methylene Blue Dye from Aqueous Solution

Ameer Q. Abed¹, Aula M. Al Hindawi^{1*} and Hasan F. Alesary^{2*}

¹Department of Chemistry, College of Education for Pure Science, University of Kerbala, Karbala, Iraq

²Department of Chemistry, College of Science, University of Kerbala, Karbala, Iraq

*Correspondence to:

Aula M. Al Hindawi
Department of Chemistry, College of
Education for Pure Science, University of
Kerbala, Karbala, Iraq
E-mail: aulamahdi@yahoo.com

Hasan F. Alesary
Department of Chemistry, College of
Science, University of Kerbala, Karbala, Iraq
E-mail: hasan.f@uokerbala.edu.iq

Received: September 01, 2022

Accepted: October 11, 2022

Published: October 13, 2022

Citation: Abed AQ, Al Hindawi AM, Alesary HF. 2022. Green Synthesis of Zinc Sulfide Nanoparticles for the Removal of Methylene Blue Dye from Aqueous Solution. *NanoWorld J* 8(3): 79-84.

Copyright: © 2022 Abed et al. This is an Open Access article distributed under the terms of the Creative Commons Attribution 4.0 International License (CC-BY) (<http://creativecommons.org/licenses/by/4.0/>) which permits commercial use, including reproduction, adaptation, and distribution of the article provided the original author and source are credited.

Published by United Scientific Group

Abstract

The growing problems of the toxicity of methylene blue (MB) dye have increased significantly in the last few years, leading to many health problems. Many purification techniques have been proposed to treat the dye before draining into the rivers. Zinc sulfide nanoparticles (ZnS) became effective in treating the released dye. This research focuses on using green synthesis to produce ZnS nanoparticles with the help of broccoli. Broccoli extract acts as a reducing and protecting agent instead of using chemical materials. The production of ZnS nanoparticles was characterized using transmission electron microscopy (TEM), field emission-scanning electron microscopy FE-SEM, Fourier-transform infrared spectroscopy (FT-IR), and X-ray diffraction techniques. An absorption band at 275 nm corresponds to the formation of ZnS nanoparticles. The band gap energy was determined from the absorption spectrum to be 3.9 eV, which is in a redshift concerning to bulk ZnS. The XRD pattern showed that ZnS particles have a cubic structure (zinc blende) with an average crystallite size of 2.57 nm. The adsorption behavior of ZnS nanoparticles was tested with MB dye and it was found that a small amount of ZnS nanoparticles (0.1 g) were able to remove 90% of the dye from an aqueous solution.

Keywords

Adsorption, Green synthesis, Methylene blue dye, Biosynthesized ZnS nanoparticles

Introduction

MB dye (tetra methylthionine chloride) is one of the most common dyes used in textiles, rubbers, pesticides, varnishes, and pharmaceuticals. The presence of this residual dye in wastewater is one of the most serious issues that attract the attention of researchers because these dyes are not biodegradable and can cause serious problems to the environment and living organisms [1, 2]. Therefore, various purification techniques have been proposed to solve this issue, for example, ozonation, and chlorination [3, 4]. Although such approaches have been used to date, they have various disadvantages. The adsorption technique was widely utilized to treat dyes [5]. Many adsorbents have been used for adsorbing methylene blue dye (MB) from water sources such as nickel alginate/activated carbon, and nickel alginate/grapheme oxide, these adsorbents have an adsorption capacity of 465.120 mg/g at 303 K and 537.630 mg/g at 303 K, respectively [6]. Activated carbon is an adsorbent that is used to remove different kinds of inorganic pollutants such as heavy and organic elements, various dyes, and phenols because of the high adsorption capacity. However, activated carbon has some limitations such as the high cost and reuse problems, as well as the difficulty of separating from

wastewater [7]. Yang's group studied the adsorption of MB dye from an aqueous solution using graphene oxide (GO), and the percentage removal of dye was found to be 99%. [8] Nano-carbon material (N-CM), which was prepared using the solvothermal method, was used as an adsorbent for cationic MB dye with an adsorption capacity of up to 118.98 mg/g. According to the authors, an electrostatic attraction formed between N-CM and MB dye [9].

Alternative and low-cost semiconductor nanomaterials have been used for water purification [10-12]. Due to the small-sized and optical properties, semiconductor nanomaterials are used either as photocatalysis or adsorbents. In this work, ZnS nanoparticles were used as an adsorbent to get rid of MB dye from aqueous solutions. Nanocrystalline zinc sulfide has interesting properties due to the size confinement effect [13, 14]. As the particle size decreases, the number of atoms in the particles decreases too, which leads to a reduction in the overlap of atoms orbitals, and consequently the widths of the valance and conduction bands narrows and the energy gap is increased; accordingly, therefore, the absorption edge will be shifted towards high energy. It is well known that zinc sulfide (ZnS) has a wide direct band gap ($E_g = 3.6$ eV at 27 °C), which emits light in the UV region of the electromagnetic spectrum [15].

Many approaches have been devoted to developing methods for the production of metal and semiconductor nanoparticles of various sizes and shapes such as sol-gel, chemical precipitation, helium droplet, biosynthetic methods, and laser deposition [16-18] ZnS nanoparticles can be prepared by, for example, thermal decomposition, microwave-assisted, chemical precipitation, and sono-chemical methods [19, 20]. Green synthesis is of particular interest since it relies on the use of biological extracts to cap, reduce, and stabilize nanoparticles [21, 22]. The broccoli plant extract was used for the first time as a capping and reducing agent to control the growth process of ZnS nanoparticles to form zinc sulfide nanoparticles because it contains many bioactive compounds such as polyphenols [23]. The resulting biosynthesized particles (B : ZnS) are believed to be biocompatible, eco-friendly, and non-toxic. Therefore, producing nanoparticles with small size and large surface-to-area ratios offers a far-reaching opportunity for use as an adsorbent to treat dyes/pollutants. Furthermore, biosynthesized ZnS particles can be used in the medical field for purposes such as drug carriers and fillings in medical substances [24].

Material and Methods

Materials

Zinc sulfate heptahydrate ($ZnSO_4 \cdot 7H_2O$) and sodium sulfide ($Na_2S \cdot xH_2O$) were purchased from CDH and used without further purification. De-ionized water was used to prepare solutions. Methylene blue dye (MB) was purchased from Sigma Aldrich.

Preparing broccoli extract

The fresh broccoli flowers were washed with tap water and then with deionized water to remove any dust. The flowers

were dried in the shade for ten days. The broccoli flowers were ground into a fine powder using a mill. To prepare the broccoli extract, 10 g of the broccoli powder was dissolved in 100 mL of deionized water. The solution was then heated for 10 min at 50°C with stirring. After that, the solution was filtered using filter paper No. 1, and the supernatant kept in fridge before using it to synthesize ZnS nanoparticles.

The bio fabrication of zinc sulfide particles

To produce ZnS particles, 0.01 M sodium sulfide ($Na_2S \cdot xH_2O$) was dissolved in 100 mL of deionized water and kept under continuous stirring for 30 min. In another beaker, 0.2875 g of zinc sulfate heptahydrate ($ZnSO_4 \cdot 7H_2O$) was dissolved in 100 mL of deionized water and stirred for 30 min. Different amounts of broccoli extract were added to the zinc sulfate heptahydrate and stirred for a few min. Sodium sulfide solution was then added slowly to the mixture and stirred for one hour. A cloudy white solution was obtained which indicated the formation of ZnS nanoparticles. Finally, the precipitate (zinc sulfide) was washed and dried.

Preparation of ZnS/MB solutions

Standard solution of MB dye (200 ppm) was prepared by dissolving 0.2 g of the dye in 1000 mL of deionized water. From these solutions, further solutions of different concentrations were prepared using the serial dilution method, as required by the experiments. To study the ability of as-prepared ZnS particles as an adsorbent, 20 mL of MB solution (5 ppm) was mixed with different amounts of bio fabricated zinc sulfide particles at 298 K. This sample was shaken for different periods of time (5-60 min) at a speed of 400 tr/min before being filtered. For the purposes of determining the wavelength (λ_{max}) at which the highest absorption of dyes occurs (MB), a solution was prepared with a specific concentration of dye, and the associated absorption spectrum recorded using a UV-Vis spectrophotometer (in the range 200-800 nm) and using standard quartz cuvette (1.0 cm square profile).

Characterization of bio fabrication of zinc sulfide particles

To characterize the crystal structure of biosynthesized ZnS nanoparticles, the X-ray diffraction (X pert pro-Panalytical) technique was utilized using Cu-K α radiation. The shape and size of the prepared ZnS nanocrystals were examined via transmission electron microscopy (JEOL JEM-2100 LaB6) and field emission scanning electron microscopy (Zeiss SIGMA VP-FESEM). ZnS particles' optical properties were studied via a UV-Vis spectrophotometer (Double Beam-1800, Shimadzu-Japan). Finally, the functional groups on the surface of ZnS particles were characterized via Fourier-transform infrared spectroscopy (FT-IR) (IRAffinity-1S instrument Shimadzu, Japan).

Results and Discussion

The appearance of a white color after mixing the starting materials with broccoli flower extract is an indicator of the formation of biosynthesized ZnS particles (B : ZnS). Another supporting evidence for the formation of ZnS particles was provided by studying the particles' optical properties. Different

amounts of broccoli extract (6 mL, 10 mL, 20 mL, and 40 mL) were chosen to identify the optimal conditions for producing small nanoparticles with a high surface-to-area ratio, while the amount of the other two precursors were kept the same (100 mL). Figure 1a shows that the absorption peaks depend strongly on the extract concentration. At a lower concentration (6 mL), no obvious peak was observed. When 10 mL of the broccoli extract was added to the solution, a significant absorption peak was seen at 275 nm, which is blue shifted with respect to the bulk ZnS (340 nm), [25] which is probably due to the quantum confinement phenomenon. At high concentrations (i.e., 20 and 40 mL), significant shifts towards lower energies were noted.

A Tauc equation [26] was used to estimate the band gap energy from the UV-Vis spectrum recorded when 10 mL of the extract was added (absorption edge of 275 nm) to zinc sulfate solution. The band gap energy (Figure 1b), which was calculated from the extrapolation of the linear curve with the x-axis, shifts towards higher energy (3.9 eV) compared to that of bulk ZnS (3.6 eV) due to the confinement of electrons at the nanoscale. The value of the band gap energy is in a good agreement with the earlier experimental work performed by Sabaghi et al. [19].

$$\alpha h\nu = C (h\nu - E_g)^n \dots\dots\dots (1)$$

Where (n) is the direct electronic transition which is equal to 0.5 [27] (α) is the absorption coefficient, h is the Plank's constant, and ν is the frequency of light. (E_g) is the band gap energy and C is the constant.

After establishing the best extract concentration that should be used in the formation of ZnS nanoparticles, the influence of pH on the production of ZnS particles was investigated. By adding either 0.1 M of HCl or 0.1 M of NaOH, several pH values (3, 5, 7, 9, 11, and 12) were selected. As shown in figure 2, a shift in the absorption edge ($\lambda = 275$ nm)

towards the high-energy region was observed at pH 5. The peaks' intensities shift towards higher wavelengths (377 nm) as the solution becomes more basic, which is higher than the absorption edge of bulk ZnS (340 nm) [25]. Furthermore, at pH 12, the absorption peak declines and becomes less than at pH 11. This might be attributed to the formation of zinc hydroxide in the solution, resulting in a decrease in Zn^{2+} ions, which consequently reduces the yield of ZnS particles.

The XRD pattern shows clear evidence of the formation of crystalline zinc sulfide nanoparticles. Three diffraction peaks appear at theta angles of 28.76°, 47.97° and 56.6° that correspond to the (111), (220), and (311) planes, respectively [28]. This finding agrees with the results obtained in recent experiments [25]. According to the Debye- Scherrer formula: [29]

$$D = K \lambda / \beta \cos\theta \dots\dots\dots (2)$$

Where "D" is the average particle size, "K" is the shape factor 0.9, " λ " is the X-ray wavelength (0.154 nm), " θ " is the Bragg's angle in radians, and " β " is the full width at half maximum (FWHM) in radians. The average crystallite size was calculated to be around 2.57 nm based on the line width analysis of the (111) diffraction plane. XRD diffraction gives an average interplanar distance of 0.22 nm, which is assigned to the zinc blende structure (cubic structure) (Figure 3).

FE-SEM images in figure 4a and b show the surface morphology of biosynthesized ZnS particles. Several spherical particles were observed during FE-SEM analysis. ImageJ software program was used to calculate the particles size [30] and it was found to be nearly 4 nm. Although broccoli extract was used as a capping agent, some agglomeration of ZnS particles was seen in the TEM image (Figure 4c). A possible interpretation is the association of ZnS particles through drying the sample before introducing it to the TEM. In addition, many small spherical particles can be seen, as shown in the expanded view.

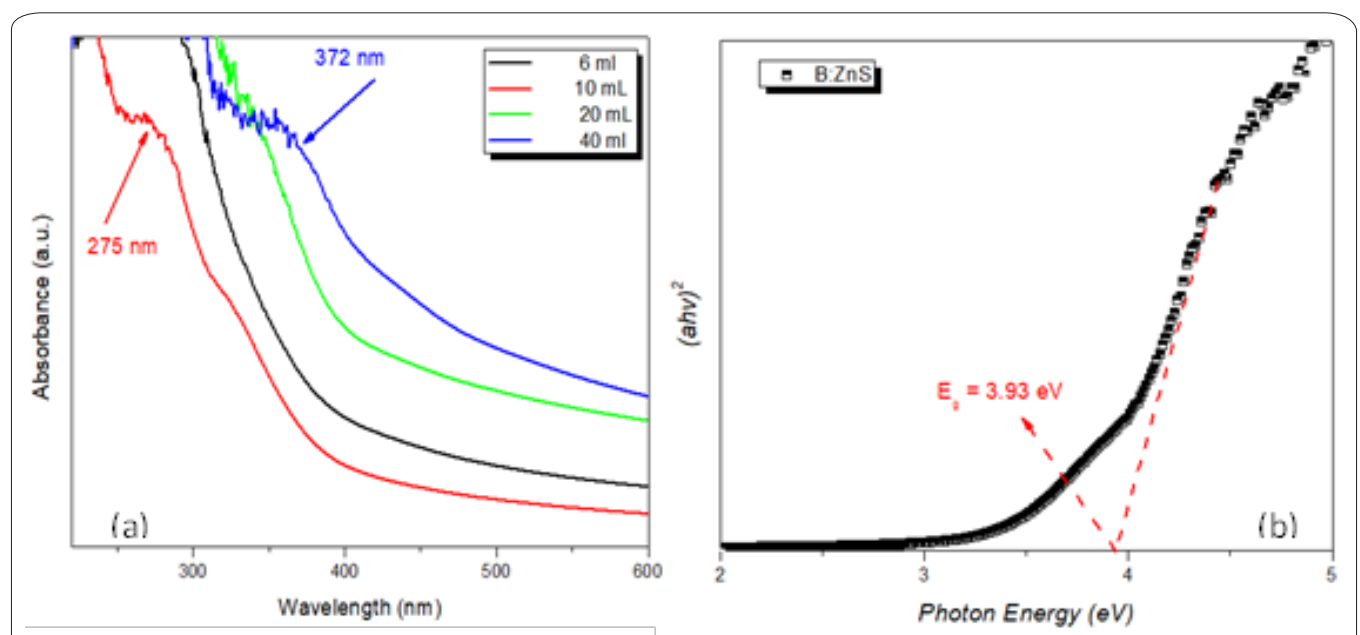


Figure 1: (a) UV-Vis spectra of zinc sulfide nanoparticles as a function of the extract concentrations after one h of shaking. (b) The band gap energy was estimated from the UV-Vis spectrum that was recorded when 10 mL of the extract was added (absorption edge of 275 nm).

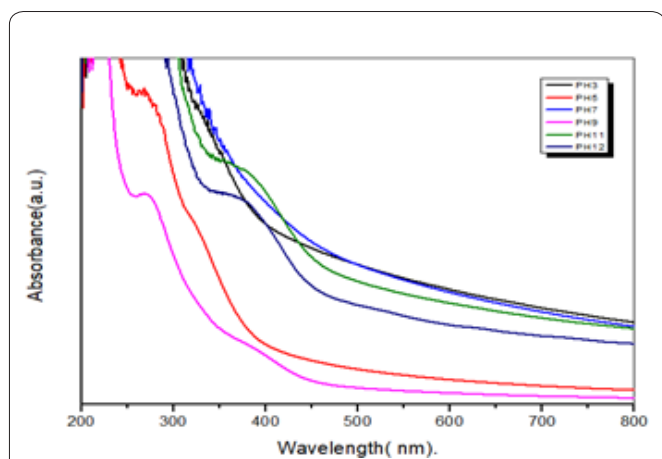


Figure 2: Illustration of the influence of pH on the absorption spectra of as-prepared ZnS nanoparticles.

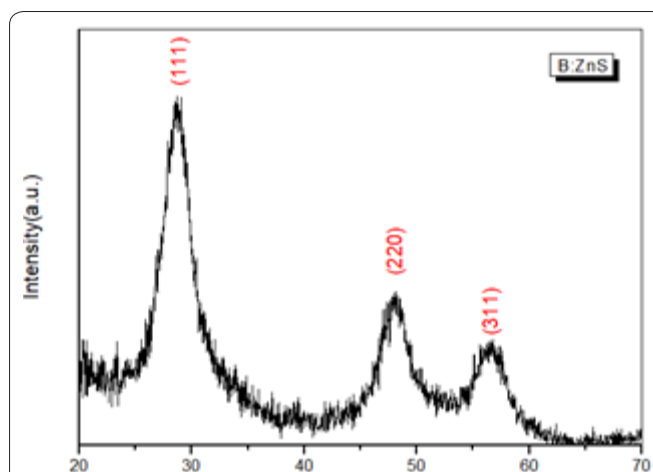


Figure 3: X-ray diffraction pattern of ZnS nanocrystals which form in the presence of 10 mL broccoli extract.

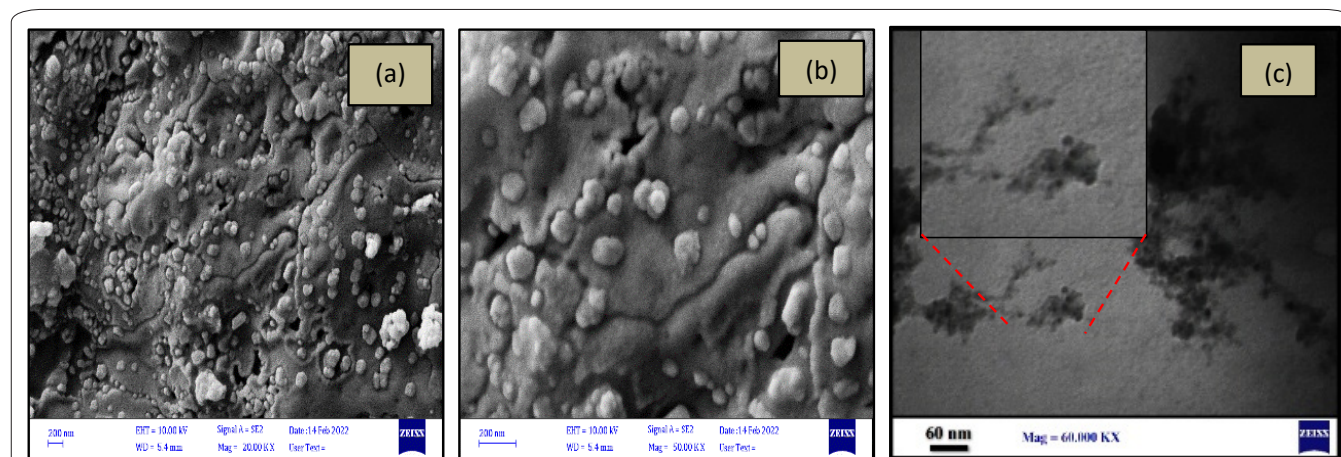


Figure 4: (a) and (b) FE-SEM images of ZnS nanoparticles formed in the presence of broccoli extract as a capping agent. (c) TEM image of ZnS nanoparticles (the extended view shows the formation of small spherical particles).

To investigate the functional groups attached to the surface of ZnS particles, an FTIR spectrum was recorded in the range of 400 - 4000 cm^{-1} . **Figure 5** shows the peaks centered at 612 and 657 cm^{-1} representing the Zn-S bond [31]. The peak at 1411 cm^{-1} is assigned to a C=C group from the aromatic conjugates from the broccoli extract [32]. The peak appears at 1640 cm^{-1} , suggesting the presence of an OH group. The broad peak around 3200 to 3500 cm^{-1} is attributed to the OH group of phenol in the extract. Sharp peaks in the range of 2330 to 2380 cm^{-1} can be assigned to the S-H bond.

The efficiency of ZnS nanoparticles as an adsorbent to remove MB dye from wastewater was investigated using UV-Vis spectrophotometry. The effect of contact time on the adsorption process was studied. **Figure 6a** shows that by increasing the contact time (5, 15, 30, and 60 min), the intensity of the MB dye peaks decreased.

The effect of changing the amount of B:ZnS of particles (0.1, 0.2, 0.3, 0.4, and 0.5 g) on the adsorption process was studied, **figure 6b** shows that MB dye has an absorption peak at 666 nm. It was noticed that a small amount of B:ZnS particles (0.1 g) adsorbs more dye compared to 0.5 g of B:ZnS

particles, which is possibly due to the decreasing surface area of particles because of the formation of a large assembly of B:ZnS when large amounts were added. The mechanism of MB adsorption onto B:ZnS nanoparticles has still not been found but according to a study about the adsorption of MB dye on magnetized *Tectona Grandis* sawdust, [33] the positive charge on the nitrogen atom of the dye will connect (electro-

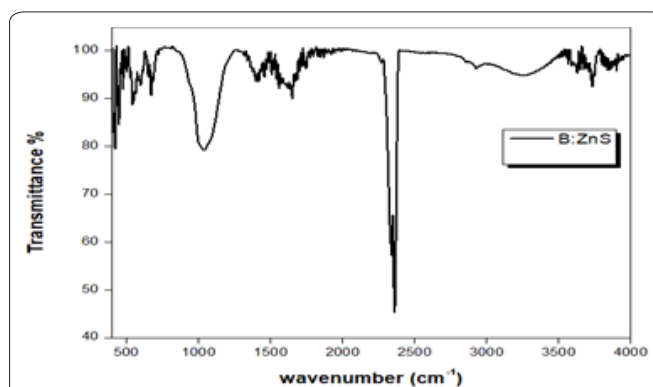


Figure 5: FTIR spectrum of ZnS nanoparticles formed in the presence of broccoli extract.

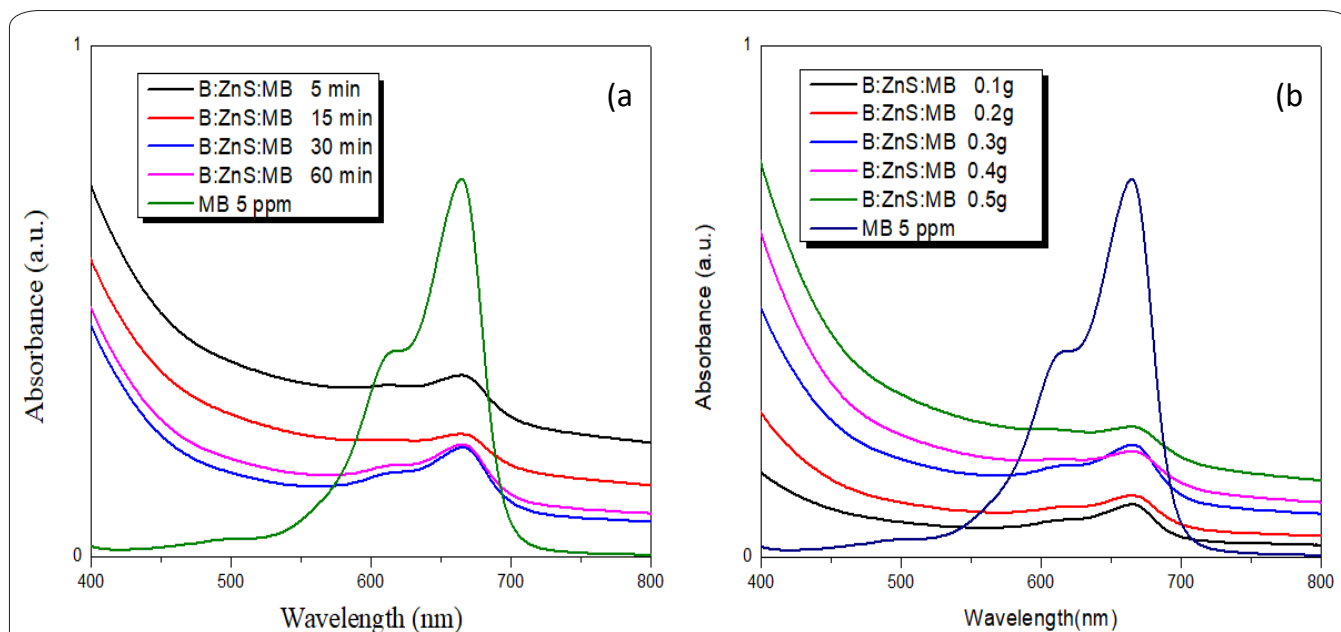


Figure 6: UV-Vis spectra of MB dye after the addition of ZnS particles formed with the presence of broccoli (B:ZnS) as a function of (a) contact time, and (b) amount of ZnS particles. The absorption band of MB dye is 666 nm.

static attraction) to the negative charge of oxygen of the bioactive compounds present in broccoli extract which is already attached to the ZnS surface.

The percentage of dye removal was obtained from the following equation:

$$\text{Dye removal \%} = \frac{(C_i - C_e)}{C_i} \times 100 \quad \dots \dots \dots (3)$$

Where C_i is the initial concentration of MB dye (mg/L), and C_e is the equilibrium concentration of MB dye after adsorption (mg/L). The best removal ratio was found to be 90%. This observation is quite similar to Albokheet's group, which found that the percentage removal of MB dye on copper oxide/Carboxymethyl cellulose nanocomposite was 92% when the concentration of the dye was 11 ppm [34].

Conclusions

This paper demonstrates the bio-green synthesis of zinc sulfide nanoparticles using broccoli flower extract. The band gap energy of biosynthesized ZnS particles increases, since the bioactive components of the extract acts as a protecting agent, which forbids the formation of large particles or masses of ZnS particles and also confirming that the ZnS particles are in the quantum confinement regime. After research, it was found that a small amount of B:ZnS particles (0.1 g) are able to adsorb methylene blue dye (MB) from wastewater with removal percentage of ~ 90%.

Acknowledgment

The authors would like to thank the University of Kerbala for providing the required materials and instruments for this work.

References

1. Affat SS. 2021. Classifications, advantages, disadvantages, toxicity effects of natural and synthetic dyes: a review. *University of Thi-Qar Journal of Science* 8(1): 130-135.
2. Verma RK, Sankhla MS, Rathod NV, Sonone SS, Parihar K, et al. 2021. Eradication of fatal textile industrial dyes by wastewater treatment. *Biointerface Res Appl Chem* 12(1): 567-587. <https://doi.org/10.33263/BRIAC121.567587>
3. Tripathi S, Hussain T. 2022. Water and wastewater treatment through ozone-based technologies, development in wastewater treatment research and processes. In: Shah M, Rodriguez-Couto S, Biswas J (eds) *Development in wastewater treatment research and processes*. Elsevier, pp 139-172. <https://doi.org/10.1016/B978-0-323-85583-9.00015-6>
4. Ghanbari S, Fatehizadeh A, Khiadani M, Taheri E, Iqbal H. 2022. Treatment of synthetic dye containing textile raw wastewater effluent using UV/Chlorine/Br photolysis process followed by activated carbon adsorption. *Environ Sci Pollut Res* 29(26): 39400-39409. <https://doi.org/10.1007/s11356-022-18860-5>
5. Jawad RA, Shiltagh N, Aboud LH, Watkins MJ. 2021. The effect of silver nanoparticles on a mixture of mb-dye/pva-polymer as determined by absorption and emission spectra measurements. *NanoWorld J* 7(1): 13-21. <https://doi.org/10.17756/nwj.2021-087>
6. Wang Y, Pan J, Li Y, Zhang P, Li M, et al. 2020. Methylene blue adsorption by activated carbon, nickel alginate/activated carbon aerogel, and nickel alginate/graphene oxide aerogel: a comparison study. *J Mater Res Technol* 9(6): 12443-12460. <https://doi.org/10.1016/j.jmrt.2020.08.084>
7. Babick F, Schießl K, Stintz M. 2011. van-der-Waals interaction between two fractal aggregates. *Adv Powder Technol* 22(2): 220-225. <https://doi.org/10.1016/j.apt.2010.11.014>
8. Yang J, Shojaei S, Shojaei S. 2022. Removal of drug and dye from aqueous solutions by graphene oxide: Adsorption studies and chemometrics methods. *NPJ Clean Water* 5(5) 1-10. <https://doi.org/10.1038/s41545-022-00148-3>
9. Liang C, Shi Q, Feng J, Yao J, Huang H, et al. 2022. Adsorption behaviors of cationic methylene blue and anionic reactive blue 19 dyes onto nano-carbon adsorbent carbonized from small precursors. *Nanomaterials (Basel)* 12(11): 1814. <https://doi.org/10.3390/nano12111814>

10. Vasantharaj S, Sathiyavimal S, Senthilkumar P, Kalpana V, Rajalakshmi S, et al. 2021. Enhanced photocatalytic degradation of water pollutants using bio-green synthesis of zinc oxide nanoparticles (ZnO NPs). *J Environ Chem Eng* 9(4): 105772. <https://doi.org/10.1016/j.jece.2021.105772>
11. Karuppasamy P, Nisha NRN, Pugazhendhi A, Kandasamy S, Pitchaimuthu S. 2021. An investigation of transition metal doped TiO₂ photocatalysts for the enhanced photocatalytic decoloration of methylene blue dye under visible light irradiation. *J Environ Chem Eng* 9(4): 105254. <https://doi.org/10.1016/j.jece.2021.105254>
12. Vinayagam R, Selvaraj R, Arivalagan P, Varadavenkatesan T. 2020. Synthesis, characterization and photocatalytic dye degradation capability of Calliandra haematocephala-mediated zinc oxide nanoflowers. *J Photochem Photobiol B* 203: 111760. <https://doi.org/10.1016/j.jphotochem.2019.111760>
13. Ramalingam G, Kathirgamanathan P, Ravi G, Elangovan T, Manivanan N, et al. 2020. Quantum confinement effect of 2D nanomaterials. In: Divsar F(ed) *Quantum dots-fundamental and applications*. IntechOpen. <https://doi.org/10.5772/intechopen.90140>
14. Choudapur V, Kapatkar S, Raju A. 2019. Structural and optoelectronic properties of zinc sulfide thin films synthesized by co-precipitation method. *Acta Chemica Iasi* 27(2): 287-302.
15. Khalil MH, Mohammed RY, Ibrahim MA. 2021. The influence of CBD parameters on the energy gap of ZnS narcissus-like nanostructured thin films. *Coatings* 11(9): 1131. <https://doi.org/10.3390/coatings11091131>
16. Al Hindawi A, Taher K, Habeeb N, Joudah I, Shiltagh N. 2020. Fabrication and characterization of silver nanoparticles using plant extract.
17. Shiltagh NM, Ridha NJ, Al Hindawi AM, Tahir KJ, Madlol RA, et al. 2020. Studying the optical properties of silver nitrates using a pulsed laser deposition technique. *AIP Conference Proceedings* 2290(1): 050059. <https://doi.org/10.1063/5.0028006>
18. Yang S, Feng C, Spence D, Al Hindawi AM, Latimer E, et al. 2017. Robust ferromagnetism of chromium nanoparticles formed in superfluid helium. *Advanced Materials* 29(1): 1604277. <https://doi.org/10.1002/adma.201604277>
19. Sabaghi V, Davar F, Fereshteh Z. 2018. ZnS nanoparticles prepared via simple reflux and hydrothermal method: Optical and photocatalytic properties. *Ceram Int* 44(7): 7545-7556. <https://doi.org/10.1016/j.ceramint.2018.01.159>
20. Wang Q, Xu P, Zhang G, Hu L, Wang P. 2019. Visible-light responsive g-C₃N₄ coupled with ZnS nanoparticles via a rapid microwave route: characterization and enhanced photocatalytic activity. *Appl Surf Sci* 488: 360-369. <https://doi.org/10.1016/j.apsusc.2019.05.238>
21. Al Hindawi AM, Joudah I, Hamzah S, Tarek Z. 2019. Plant extract: safe way for fabrication silver nanoparticles. *IOP Conf Ser: Mater Sci Eng* 571: 012069. <https://doi.org/10.1088/1757-899X/571/1/012069>
22. Turki ZT, Al Hindawi AM, Shiltagh NM. 2022. Green synthesis of CdS nanoparticles using avocado peel extract. *NanoWorld J* 8(3): 73-78. <https://doi.org/10.17756/nwj.2022-102>
23. Córdova C, Vivanco JP, Quintero J, Mahn A. 2020. Effect of drum-drying conditions on the content of bioactive compounds of broccoli pulp. *Foods* 9(9): 1224. <https://doi.org/10.3390/foods9091224>
24. Sathishkumar M, Subiraminiyam N, Sasikumar M. 2017. Antibacterial activities of zinc sulphide nanoparticles using leaf extract of Lawsonia inermis. *Neburu E-Journal* 5(1): 17-21.
25. Hamed ZH, Ahmed KEA, Elsheikh HA. 2021. Synthesis and characterization of ZnS nanoparticles by chemical precipitation method. *Aswan University Journal of Environmental Studies (AUJES)* 2(2): 147-154.
26. Makuła P, Pacia M, Macyk W. 2018. How to correctly determine the band gap energy of modified semiconductor photocatalysts based on UV-Vis spectra. *J Phys Chem Lett* 9(23): 6814-6817. <https://doi.org/10.1021/acs.jpcclett.8b02892>
27. Marcolongo D, Nocito F, Ditaranto N, Aresta M, Dibenedetto S. 2020. Synthesis and characterization of pn junction ternary mixed oxides for photocatalytic coprocessing of CO₂ and H₂O. *Catalysts* 10(9): 980. <https://doi.org/10.3390/catal10090980>
28. Naeimi H, Kiani F, Moradian M. 2018. Rapid microwave promoted heterocyclization of primary amines with triethyl orthoformate and sodium azide using zinc sulfide nanoparticles as recyclable catalyst. *Green Chem Lett Rev* 11(3): 361-369. <https://doi.org/10.1080/17518253.2018.1510990>
29. Mustapha S, Ndamitso M, Abdulkareem A, Tijani J, Shuaib D, et al. Comparative study of crystallite size using Williamson-Hall and Debye-Scherrer plots for ZnO nanoparticles. *Adv Nat Sci Nanosci Nanotechnol* 10: 045013.
30. Rasband WS. 2011. ImageJ. [<http://imagej.nih.gov/ij/>] Accessed on October 13, 2022.
31. Othman RS, Omar RA, Omar KA, Ghani AI, Ahmad RQ, et al. 2019. Synthesis of zinc sulfide nanoparticles by chemical coprecipitation method and its bactericidal activity application. *Polytechnic Journal* 9(2): 156-160. <https://doi.org/10.25156/ptj.v9n2y2019.pp156-160>
32. Osuntokun J, Onwudiwe DC, Ebenso EE. 2019. Green synthesis of ZnO nanoparticles using aqueous *Brassica oleracea* L. var. italica and the photocatalytic activity. *Green Chem Lett Rev* 12(4): 444-457. <https://doi.org/10.1080/17518253.2019.1687761>
33. Ahmed M, Mashkoo F, Nasar A. 2020. Development, characterization, and utilization of magnetized orange peel waste as a novel adsorbent for the confiscation of crystal violet dye from aqueous solution. *Groundw Sustain Dev* 10: 100322. <https://doi.org/10.1016/j.gsd.2019.100322>
34. Albokheet W, Gouda M, Alfaiyz Y. 2021. Removal of methylene blue dye using copper oxide/carboxymethyl cellulose nanocomposite: kinetic, equilibrium and thermodynamic studies. *Asian Journal of Advances in Research* 8(1): 1-18.